

Spontaneous Rotation, Multiply Charged Vortices, and the Kelvin-Helmholtz Instability in Nonconservative Trapped Bose Condensates

Samuel N. Alperin¹ and Natalia G. Berloff^{2, 1, *}

¹*Department of Applied Mathematics and Theoretical Physics,
University of Cambridge, Cambridge CB3 0WA United Kingdom*

²*Skolkovo Institute of Science and Technology, Bolshoy Boulevard 30, bld.1, Moscow, 121205, Russian Federation*

The existence of quantized vortices is a key feature of Bose-Einstein condensates. In equilibrium condensates only quantum vortices of unit topological charge are stable, due to the dynamical instabilities of multiply charged defects, unless supported by strong external rotation. In this Letter we elucidate the formation, stability, coalescence and interactions of bound vortex states in trapped nonequilibrium Bose condensates such as exciton-polariton condensates pumped in a ring geometry. These bound states consist of like-signed vortices which share a single core, but whose singularities are spatially separated within the core. We propose that they may form spontaneously during the condensate formation or externally imprinted and stabilized by the particle fluxes towards the condensate center, which is a stark contrast with instability of multiply charged vortices in equilibrium condensates. We show that the maximum topological charge of these states is limited by the Kelvin-Helmholtz instability, and, therefore, by the condensate radius and pumping intensity. We show that multiply charged vortices in trapped nonconservative condensates become promising testbeds for analog gravity and for studying the fundamental physics of multiply charged vortices in quantum fluids.

Significance Statement- The quantization of vorticity is a fundamental feature of quantum fluids, and the vortex structure and dynamics are of intense interest. However, vortices with more than a single quanta of rotation are notoriously difficult to create.. Given their promise as test-beds for fundamental physical phenomena, much effort has been exerted towards the creation of stable vortices of greater-than-unit charge. In this report we introduce conditions under which stable multiply charged vortices form by themselves in trapped nonequilibrium Bose condensates, and elucidate the properties of these new fundamental structures. In particular, we discover that multiply charged quantum vortices emit characteristic acoustic radiation, tend to merge together, and respond to the Kelvin-Helmholtz instability by decreasing their charge.

Introduction- From their macroscopic coherence it follows that Bose Einstein condensates (BECs) may only support rotational flow in the form of quantized vortices [1]. These vortices are thus topological in nature, and are characterized by a phase rotation of integer (ℓ) steps of 2π around a phase singularity. However, while in principle quantized vortices may take on any topological charge, in practice it is understood that only vortices of charge $\ell = \pm 1$ are dynamically stable: higher order vortices quickly shatter into constellations of unit vortices due to energetics of the system. This shattering process has been detailed theoretically and observed experimentally in the context of stationary, harmonically trapped atomic BECs [2–4]. The case is somewhat different for superharmonically trapped, rapidly rotated condensates,

for which there exists a critical rotation rate above which the vorticity of the system becomes concentrated within a single effective core. This state, in which all vorticity is within a single effective core, has been called the *giant vortex* state by its first experimental observers [5, 6]. Such giant vortex is, therefore, may be different from a state in which there is a single point singularity with topological charge magnitude greater than one – *multiply charged vortex*, however, in practice it is often impossible to distinguish between the two. On the one hand, the density in the vortex core is negligible, which hinders the resolution of singularity. On the other hand, the structure of interest is hydrodynamical, and thus only has meaning up to the length scales for which the hydrodynamical treatment applies. The classical field description being a long wavelength approximation of something which is in reality granular and nonclassical, the hydrodynamic description only applies down to the healing length. Singularities of like charge which are bound to within a healing length are thus, to any probe in the hydrodynamical regime, indiscernible from the theoretical *multiply charged vortex*. Thus from here on we find it useful to call all such vortex structures *multiply charged*.

In our study we focus on a BEC away from the thermodynamical equilibrium supported by continuous gain and dissipation such as polariton [7], photon [8] or magnon [9, 10] condensates. To be more specific we use the example of polariton condensate however the results reported may be relevant to other nonequilibrium condensates. The exciton-polariton (polariton) is a bosonic quasiparticle composed of light (photons) and matter (excitons). Polaritons can be generated in optical semiconductor microcavities. In a typical experimental system, laser light is continuously pumped into the cavity to excite excitons (bound electron-hole pairs) in a semiconductor sample.

* correspondence address: N.G.Berloff@damtp.cam.ac.uk

The photons remain trapped in the cavity for some time, repeatedly being absorbed by the semiconductor to excite excitons, and then being re-emitted as the excitons decay. The excitons form superposition states (polaritons) with the photons, which behave neither as light or matter. Due to the finite confinement times of the cavity photons, the polaritons in the condensate are themselves short lived. In this way the polariton condensate is fundamentally different from other condensates: here neither energy nor particle number need be conserved. Thus while a polariton condensate may settle into a *steady state* (a state in which the wavefunction is time invariant up to a global phase shift), such a state is one in which dissipation is balanced by particle gain. The corollary is that steady state flows are possible. It is well understood that the pattern forming capabilities of nonequilibrium, nonconservative systems is richer than those of equilibrium, conservative systems [11], making the polariton condensate a fascinating object with which to explore the possibility of novel quantum hydrodynamical behaviors [12].

In this Letter, we show theoretically that giant vortex and multiply charged vortex states can appear spontaneously and remain throughout the coherence time in a BEC of exciton-polariton quasiparticles excited by a ring-shaped laser profile, without the application of any external rotation, trapping potentials, or stirring. Previously, the spontaneous formation of a giant vortices of a given charge has been theoretically proposed and experimentally realised in polariton condensates by pumping in an odd number of spots around a circle [13]. The central vortex in this geometry is created driven by the antiferromagnetic coupling of the neighboring condensates and the frustration arising from their odd number. The multiply charged vortices we discuss in our Letter differ from that work in the geometry considered (ring-pumped trapped condensates, long coherence times), formation mechanism (probabilistic and spontaneous during condensation) and the vortex properties (vortices exist on the maximum density background and so are truly nonlinear in nature). We describe their formation, stability, and dynamics. The dynamics of two and more interacting multiply charged vortices are also studied. We find that our results apply for a wide range of possible experimental parameters, suggesting that these structures are general to ring-pumped trapped polariton BECs.

The dynamics of the polariton BEC in the mean field are described by the complex Ginzburg-Landau equation (cGLE) coupled to a real reservoir equation representing the bath of hot excitons in the sample, nonresonantly excited by the spatially resolved laser pump profile $P(\mathbf{r})$ [14–16]

$$i\partial_t\psi = -\frac{\hbar^2}{2m}(1-i\hat{\eta}N_R)\nabla^2\psi + U_0|\psi|^2\psi + g_RN_R\psi \quad (1)$$

$$+ \frac{i\hbar}{2}(R_RN_R - \gamma_C)\psi + V_{\text{ext}}\psi + i\bar{P}\psi^{*(n-1)} \quad (2)$$

$$\partial_tN_R = P - (\gamma_R + R_R|\psi|^2)N_R. \quad (2)$$

in which ψ represents the condensate wavefunction, N_R and the exciton reservoir density. U_0 and g_R give the polariton-polariton and exciton-polariton interaction strengths, R_R and $\hat{\eta}$ represent the scattering and diffusion rates. The effective mass of the polariton is given by m . Finally, the loss rates of excitons and polaritons are described by γ_C and γ_R . To rewrite these equations in a more amenable, nondimensional form, we employ the transforms $\psi \rightarrow \sqrt{\hbar R_R/2U_0l_0^2}\psi$, $t \rightarrow 2l_0^2t/R_R$, $r \rightarrow \sqrt{\hbar l_0^2/(mR_R)}r$, $N_R \rightarrow N_R/l_0^2$, $P \rightarrow R_R P/2l_0^2$, and we define the nondimensionless parameters $g = 2g_R/R_R$, $b_0 = 2\gamma_R l_0^2/R_R$, $b_1 = \hbar R_R/U_0\eta = \hat{\eta}/l_0^2$, $\gamma = \gamma_C l_0^2/R_R$, and $\gamma = \gamma_C l_0^2/R_R$, where we set $l_0 = 1\mu\text{m}$. This yields [17]

$$i\partial_t\psi = -(1-i\eta N_R)\nabla^2\psi + |\psi|^2\psi + gN_R\psi \quad (3)$$

$$+ i(N_R - \gamma)\psi \quad (3)$$

$$\partial_tN_R = P - (b_0 + b_1|\psi|^2)N_R, \quad (4)$$

Polaritons can be confined all-optically by shaping the excitation laser beam. By using spatial light modulators to shape the optical excitation, ring shaped confinements were generated with condensates forming inside the ring [18, 19]. Long-lifetime polaritons in ring traps are emerging as a platform for studies of fundamental properties of polariton condensation largely decoupled from the excitonic reservoir and, therefore, having significantly larger coherence times [20–23]. We represent the profile of the ring pump by a Gaussian annulus of the form $P(r, \theta, t) = Pe^{-\alpha(r-r_0)^2}$, which excites local quasi-particles which then flow outward. The closed-loop pump geometry has two major implications. The first is that the condensation threshold is first achieved not where the sample is pumped, but *within* the borders of the pumping ring. This results in the spatial separation of Eqs. (3–4), which makes the parameters related to the excitonic reservoirs such as b_0 , b_1 , and g irrelevant to the condensate dynamics up to a change of pump strength. The second and most critical implication of the ring pump geometry is the existence of constant fluxes towards the centre of the ring. Such fluxes carry the matter together with spontaneously formed vortices and force vortices to coalesce.

It is well known that vortices can form during the rapid condensation of a Bose gas, via the Kibble-Zurek mechanism [24–33]. However, in our system there exist a different mechanism of spontaneous defect generation in our system, which requires a relatively *slow* condensate formation. Due to the inward flow of particles in our system, the condensation threshold is reached first in the

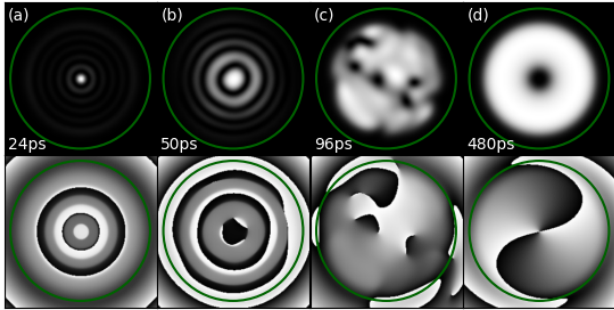


FIG. 1. Spontaneous formation of a multiply charged quantum vortex in a ring pumped polariton condensate by numerical integration of Eqs. (3-4). Density (top row) and phase (bottom row) snapshots are shown at various stages of the condensate formation. At the beginning of the condensate formation; due to the pump geometry, matter wave interference leads to annular zeros in the wavefunction (a). These ring singularities are unstable to dynamical instability, and can be observed to break into more stable unit vortices in (b) as the condensate continues to develop. The condensate fills a disk shaped region with near uniformity within the ring pump, but remaining vortices interact chaotically in (c). The vortex turbulence eventually decays, leaving a net topological charge. Repeating these simulation with different random initial conditions, the magnitude and sign of the final vorticity varies. Here $P = 5$ and $r_0 = 11.5\mu\text{m}$.

center of the system. Assuming a large enough ratio of new particle flow to dissipation, this young condensate will grow into a relatively uniform disk within the boundary of the pump. However, in between these two stages, radial matter wave interference is to be expected, with higher frequency during the early stages of condensation. The zeros of the radial interference pattern are well studied under a different name: the dark ring soliton [11, 34, 35]. As has been shown previously, these dark solitons are unstable to transverse ('snake') perturbations, and break apart into pairs of unit vortices of opposite charge [36, 37]. Thus for a slowly condensing system, it is reasonable to expect that these solitons have enough time to break down to produce a chaotic array of vortex singularities. This process resembles a two-dimensional case of the collapsing bubble mechanism of vortex nucleation [38]. As the condensation process completes and the vortex turbulence decays, there is some finite chance of the condensate being left with a net topological charge, as vortex pairs may unbind near the boundary and one or the other may leave to bind with its image. These like-charged vortices would then coalesce in the center of the condensate.

Direct numerical integration of Eqs. (3-4) not only confirms that this process can take place, but that for low pump power, the condensate takes on a net topological charge more often than not [39]. We reiterate that this coalescence of vortices is despite the lack of any external potential, external rotation, or nonuniform sample. Re-

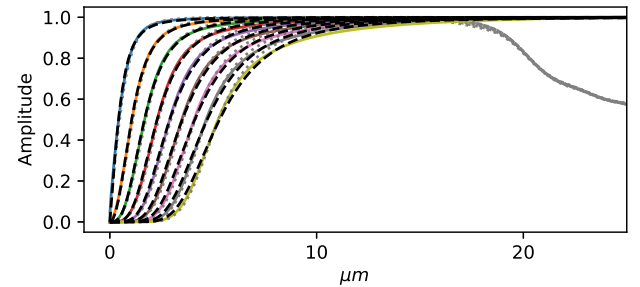


FIG. 2. Wavefunction amplitude cross sections $\sqrt{\rho(r)}$ of giant vortices of topological charge $\ell \in 1, 2.., 9$, taken from the numerical integration of Eqs. (6) (solid color), fits Eq. (7) (dashed black, approximated by the dependencies $n(\ell) = (1.1)\ell^{1.6} - 2.8$ and $w(\ell) = 2.3 + (0.6)\ln(\ell)$). Also shown are the amplitude cross-sections from direct numerical integration of Eqs. (3-4) (normalized) for $r_0 = 20\mu\text{m}$, $P = 12$, and $\gamma = 0.3$ (dotted black). In the full simulation (dotted gray), the decay of the condensate near the pump ($20\mu\text{m}$) is apparent.

peating the numerical experiment with many iterations of random initial wavefunction noise, we find multiply charged vortex states of stochastic sign and magnitude. The average topological charge magnitude is found to depend significantly on the radius of the pump ring, increasing for larger radii. An example of these dynamics is presented in Fig. 1, which shows the main steps in the process by which the condensate spontaneously adopts a topological charge of two: the formation of a central condensate surrounded by annular discontinuities in Fig. 1(a), the breakdown of an annular discontinuity into vortex pairs in Fig. 1(b), vortex turbulence in Fig. 1(c), and the final bound vortex state Fig. 1(d). For Fig. 1 we use the system parameters $\eta = 0.3$, $\gamma = 0.05$, $g = 1$, $b_0 = 1$, $b_1 = 6$, but the result was found not to depend sensitively on these choices; up to a rescaling of pump strength this behavior was reconfirmed for a large range of sample parameters: $g \in [0.1 - 2]$, $b_0 \in [0.01 - 10]$, for $\gamma \in [0.05 - 0.1]$, and for all reasonably physical values of η (including $\eta = 0$.)

An advantage in spatially separating the condensate from the reservoir in ring pumped geometry is in the enhanced coherence time that exceeds the individual particle lifetime by three orders of magnitude [40]. Therefore, spontaneously created multiply charged vortices can be observed in single shot experiments within one condensate realisation. Another way to study the multiply charged vortices is to imprint them explicitly upon a fully formed, uniform condensate [41]. This allows for the study of the structure and dynamics of carefully controlled systems of vortices. To model the result of experimental pulsed phase imprinting, we first model the formation of fully developed non-singular condensate disks. To prevent the spontaneous formation of vortices by the process described above, a relatively strong pump amplitude is used, so that the condensate forms too quickly

for the decay of ring-singularities into vortices. After the background condensate is formed, phase singularities are imprinted instantaneously and their dynamics is observed. To first understand the structure of isolated giant and multiply charged vortices, we imprint a series of condensates with different topological charges, and allow these structures to form steady states. When imprinted in equilibrium BEC, multiply charged vortices quickly break into vortices of a single unit of quantization [42].

From the spatial separation of the condensate and the reservoir, the reservoir density is negligible near the central core of the giant vortex, so that Eq. (3) takes the familiar form of the damped nonlinear Schrödinger equation (dNLSE): $i\partial_t\psi = -\nabla^2\psi + |\psi|^2\psi - i\gamma\psi$.

Under the Madelung transformation $\psi = \mathcal{A}\exp[iS - i\mu t]$ where μ is the chemical potential, the velocity is the gradient of the phase S : $\mathbf{u} = \nabla S$ and the density is $\rho(r) = \mathcal{A}^2$, the imaginary part of the dNLSE yields $\nabla \cdot (\rho\mathbf{u}) = -\gamma\rho$. Except for a narrow spatial region where the density heals itself from zero to the density of the vortex free state the density is almost a constant, so the radial component of the velocity becomes $u_r = -\gamma r$. The real part of the dNLSE reads

$$\partial_r^2\mathcal{A} + \partial_r\mathcal{A}/r + (\mu - \mathbf{u}^2 - \mathcal{A}^2)\mathcal{A} = 0, \quad (5)$$

which coincides with the corresponding steady state equation for the equilibrium condensates where velocity profile plays the role of the external potential. We therefore expect the structure of the vortices to be similar to those in equilibrium condensates with the external potential given by \mathbf{u}^2 . Close to the centre of the condensate the velocity becomes

$$\mathbf{u} = -\gamma r\hat{r} + \frac{\ell}{r}\hat{\theta},$$

where \hat{r} and $\hat{\theta}$ are unit vectors in polar coordinates. When this expression for \mathbf{u} is substituted into Eq. (5) it becomes the equation on the vortex amplitude in the centre of the harmonic trap, where γ characterises the frequency of the “trap.” In the vortex core, for small r , the centrifugal velocity dominates the radial velocity, so the equation on the rescaled amplitude $A = \mathcal{A}/\sqrt{\mu}$ with $\tilde{r} = \sqrt{\mu}r$ becomes

$$\partial_{\tilde{r}^2}A + \partial_{\tilde{r}}A/\tilde{r} + \left(1 - \frac{\ell^2}{\tilde{r}^2} - A^2\right)A = 0. \quad (6)$$

The profiles A take the approximate form

$$A = \frac{\tilde{r}^{|\ell|}}{(\tilde{r}^n + w)^{|\ell|/n}}, \quad (7)$$

with parameters w and n in which we incorporated the power expansion behaviour of the amplitude $A \sim \tilde{r}^{|\ell|}$ as $\tilde{r} \rightarrow 0$. Figure 2 shows the amplitude cross-section profiles of stable giant vortices with different topological charges $\ell \in \{1, 2, \dots, 10\}$ as the solutions of Eq. (6), along with Eq. (7).

Next we consider the arrangements of multiple giant vortices imprinted away from the trap center and brought

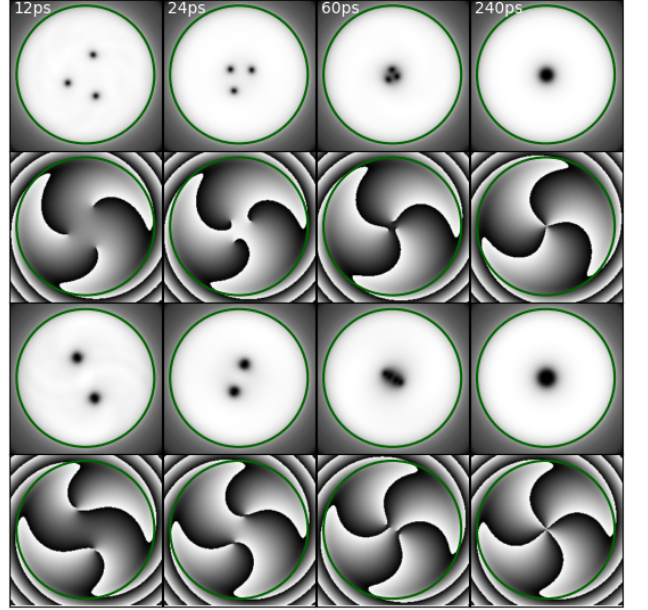


FIG. 3. From Top: Density (first row) and phase (second row) resolved dynamics of three unit vortices of like charge in a condensate formed within the boundary of an annular pump (green). Over time, the three vortices approach each other in an inward spiral, eventually merging to an inter-singularity length scale less than the healing length of the condensate. Density (3rd row) and phase (4th row) of two second-order vortices (each having topological charge $n = 2$), which over time merge into a single fourth-order vortex. Here $P = 10$ and $r_0 = 15\mu m$.

together by the radial fluxes. Fig. 3 shows two examples of the coalescence dynamics of imprinted phase defects. In the first case, three unit vortices coalesce while moving in inward spirals towards the center of the condensate, where there is no net lateral flow. In the second case, which shows the coalescence of two doubly charged vortices, it is observed that both doubly charged vortices hold together for a while before merging in the center to form a single vortex of multiplicity four. These results are found to be repeatable for a wide range of system parameters, suggesting that this behaviour is to be expected for any system parameters which allow the formation of the trapped condensate within a ring pump.

The process of coalescence of two or more vortices is interesting from the point of view of analog gravity and “cosmology in the lab” and the analogies can be drawn to the collision of two or more black stars [43–46]. As two (or more) vortices merge while spiralling around the center they excite density waves in the otherwise uniform background fluid. These acoustic excitations are long lived, and take on a frequency set by the angular frequency of the vortex spiral. For well separated vortices, this frequency increases consistently as time progresses and their separation shrinks. However, as the vortices begin to share a core these dynamics become even more

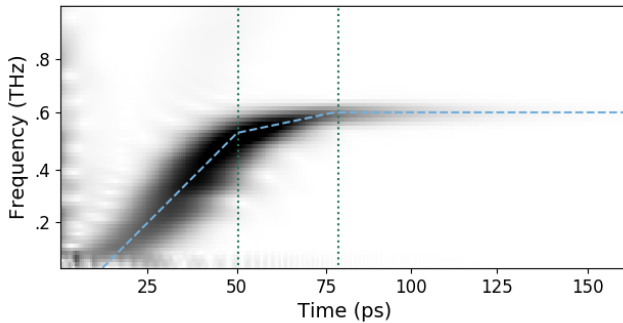


FIG. 4. Relative amplitude of density waves radiated by the approach and merger of two unit vortices, resolved in time-frequency space. Vertical lines mark the time of transition from well separated vortices to vortices sharing a common low-density core (giant vortex) (left) and the time of transition from giant vortex to multiply charged vortex (right). The three regimes of vortex matter (separated, giant vortex, multiply charged vortex) are found to have distinct acoustic radiation signatures. The ring pump radius is $20\mu\text{m}$. One vortex is imprinted at the condensate center, and the other at a distance of $18\mu\text{m}$ from the center.

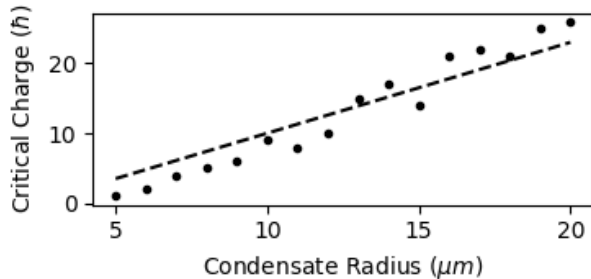


FIG. 5. Plotted is the critical topological charge at which the KHI sets in, as a function of pump radius. This is obtained by the direct numerical simulations of Eqs. (3-4). The dashed line represents the theoretical expectation of Eq. 8.

complicated and the new physics dominated by the processes in the vortex core emerges [47].

Figure 4 shows the relative amplitudes of the density waves radiated during the motion of two vortices of unit charge imprinted with a large initial separation. The average frequency of acoustic radiation is found to increase with time at a fixed rate until the vortices enter the giant vortex regime (left vertical line). During the giant vortex phase, the frequency distribution narrows and the average radiation frequency increases linearly at a much lower rate than in the well-separated vortex regime. This continues until the transition from giant vortex to multiply

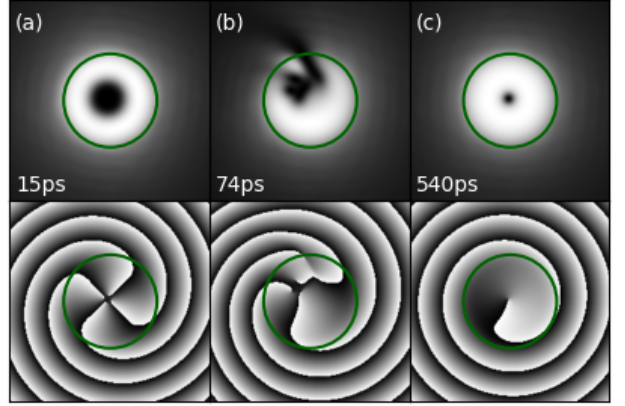


FIG. 6. For a great enough topological charge (compared to the size of the condensate), the rotational flow at the boundary of the condensate reaches the critical velocity for the Kelvin-Helmholtz instability to set in, which results in the reduction of topological charge via the nucleation of new vortices, with charges opposite to that of the giant vortex and further pair annihilation. Shown are density (top) and phase (bottom) still frames from a direct simulation of Eqs. Eqs. (3-4) exhibiting this process (radius $7\mu\text{m}$, $P = 10$). The initial topological charge is imprinted one quanta at a time, and the dynamics observed. After the fourth quanta of rotation is imprinted, the system loses stability and expels some rotation through the KHI mechanism, ending with unit topological charge.

charged vortex (right vertical line), after which a narrow band of acoustic radiation is emitted. This demonstrates that the difference between the giant vortex state and the multiply charged vortices is more than theoretical; these are physically distinct states with measurably distinct behaviors. These acoustic excitations are not unlike the gravitational waves found in the case of binary astronomical systems, which also exhibit a three stage signature in their coalescence [43].

We find that multiply charged vortices of increasing topological charge have characteristic acoustic resonances of decreasing frequency, all in the near-terahertz regime. Once the multiply charged vortex has formed and is allowed to settle, low energy density perturbations can be applied to the condensate. To model this, we simulate the effect of a small Gaussian laser pump pulse centered on the vortex. The observed effect is the emission of an acoustic energy pulse at the characteristic frequency of the vortex. As in any physical system there exist many small perturbations due to intrinsic disorder, it is likely that multiply charged vortices in a real system are regularly being excited and emitting their characteristic acoustic radiation.

Kelvin-Helmholtz instability. Next we will establish the limit on the vortex multiplicity that the trapped condensate can support. This limit is set by the maximum counterflow velocity that can be supported between the condensate and the reservoir, therefore, is determined by

the onset of a Kelvin-Helmholtz instability (KHI). KHI is the dynamical instability at the interface of two fluids when the counterflow velocity exceeds a criticality. It appears in variety of disparate systems, both classical and quantum, but has never been discussed in the context of the polaritonic systems. In quantum fluids KHI manifests itself via nucleation of vortices at a counterflow velocity exceeding the local speed of sound $v_c = \sqrt{\frac{U_0 \rho}{m}}$. It has been extensively studied for the interface between different phases of ^3He [48], two components in atomic BECs [49] or for the relative motion of superfluid and normal components of ^4He [50, 51]. In trapped condensates considered here, the counterflow is that between the condensate of radius R (which rotates with velocity $\frac{\hbar}{m} \frac{|\ell|}{R}$), and the reservoir particles along the ring, that are stationary. Thus it is expected that KHI should be initiated when the topological charge of the giant vortex state is high enough so that the condensate at the ring pump radius reaches v_c . Thus the maximum topological

charge ℓ_c allowed in one of our condensates is set by

$$|\ell_c| = \frac{\sqrt{R^2 m U_0 \rho}}{\hbar}. \quad (8)$$

Fig. 5 shows Eq. 8 (dashed line) along with the critical topological charges found in direct numerical integration of Eqs. (3-4) (dots). In these numerical experiments, we begin with a fully developed, vortex-free condensate. A unit topological charge is imprinted in the center of the condensate, and the system is allowed to settle, before another unit charge is added. This process is repeated until the onset of the KHI leads to the vortex nucleation followed by annihilation of vortex pairs and, therefore, by the reduction in the topological charge of the system. This dynamical process is shown in Fig. 6.

In conclusion, we have shown that exciton-polariton condensates excited by an annular pump can spontaneously rotate despite no external potential or application of any angular momentum, forming giant vortex and multiply charged vortices. The formation, dynamics and structure of these vortices were studied. It was also shown spectroscopically that the giant vortex to multiply charged vortex transition represents a physically meaningful state change.

[1] R. P. Feynman, in *Progress in low temperature physics*, Vol. 1 (Elsevier, 1955) pp. 17–53.

[2] S. Inouye, S. Gupta, T. Rosenband, A. Chikkatur, A. Görlitz, T. Gustavson, A. Leanhardt, D. Pritchard, and W. Ketterle, *Physical Review Letters* **87**, 080402 (2001).

[3] Y.-i. Shin, M. Saba, M. Vengalattore, T. Pasquini, C. Sanner, A. Leanhardt, M. Prentiss, D. Pritchard, and W. Ketterle, *Physical review letters* **93**, 160406 (2004).

[4] P. Engels, I. Coddington, P. Haljan, V. Schweikhard, and E. A. Cornell, *Physical review letters* **90**, 170405 (2003).

[5] U. R. Fischer and G. Baym, *Physical review letters* **90**, 140402 (2003).

[6] A. L. Fetter, B. Jackson, and S. Stringari, *Physical Review A* **71**, 013605 (2005).

[7] J. Kasprzak, M. Richard, S. Kundermann, A. Baas, P. Jeambrun, J. Keeling, F. Marchetti, M. Szymańska, R. André, J. Staehli, *et al.*, *Nature* **443**, 409 (2006).

[8] J. Klaers, J. Schmitt, F. Vewinger, and M. Weitz, *Nature* **468**, 545 (2010).

[9] V. Demidov, O. Dzyapko, S. Demokritov, G. Melkov, and A. Slavin, *Physical review letters* **100**, 047205 (2008).

[10] P. Nowik-Bolyk, O. Dzyapko, V. Demidov, N. Berloff, and S. Demokritov, *Scientific reports* **2**, 482 (2012).

[11] L. M. Pismen, *Patterns and interfaces in dissipative dynamics* (Springer Science & Business Media, 2006).

[12] S. N. Alperin and N. G. Berloff, arXiv preprint arXiv:1905.11042 (2019).

[13] K. Kalinin, M. Silva, J. D. Töpfer, W. Langbein, N. G. Berloff, and P. G. Lagoudakis, arXiv preprint arXiv:1710.03451 (2017).

[14] I. Carusotto and C. Ciuti, *Reviews of Modern Physics* **85**, 299 (2013).

[15] M. Wouters and I. Carusotto, *Physical review letters* **99**, 140402 (2007).

[16] J. Keeling and N. G. Berloff, *Physical review letters* **100**, 250401 (2008).

[17] K. P. Kalinin and N. G. Berloff, *Physical review letters* **121**, 235302 (2018).

[18] P. Cristofolini, A. Dreismann, G. Christmann, G. Franchetti, N. Berloff, P. Tsotsis, Z. Hatzopoulos, P. Savvidis, and J. Baumberg, *Physical review letters* **110**, 186403 (2013).

[19] A. Askopoulos, H. Ohadi, A. Kavokin, Z. Hatzopoulos, P. Savvidis, and P. Lagoudakis, *Physical Review B* **88**, 041308 (2013).

[20] Y. Sun, P. Wen, Y. Yoon, G. Liu, M. Steger, L. N. Pfeiffer, K. West, D. W. Snoke, and K. A. Nelson, *Physical review letters* **118**, 016602 (2017).

[21] A. Askopoulos, K. Kalinin, T. C. H. Liew, P. Cilibrizzi, Z. Hatzopoulos, P. G. Savvidis, N. G. Berloff, and P. G. Lagoudakis, *Physical Review B* **93**, 205307 (2016).

[22] L. Pickup, K. Kalinin, A. Askopoulos, Z. Hatzopoulos, P. Savvidis, N. G. Berloff, and P. Lagoudakis, *Physical review letters* **120**, 225301 (2018).

[23] S. Alyatkin, J. D. Töpfer, A. Askopoulos, H. Sigurdsson, and P. G. Lagoudakis, arXiv preprint arXiv:1907.08580 (2019).

[24] T. W. Kibble, *Journal of Physics A: Mathematical and General* **9**, 1387 (1976).

[25] T. W. Kibble, *Physics Reports* **67**, 183 (1980).

[26] W. H. Zurek, *Nature* **317**, 505 (1985).

[27] W. H. Zurek, *Physics Reports* **276**, 177 (1996).

[28] B. Damski and W. H. Zurek, *Physical review letters* **104**,

160404 (2010).

[29] C. Bäuerle, Y. M. Bunkov, S. Fisher, H. Godfrin, and G. Pickett, *Nature* **382**, 332 (1996).

[30] V. Ruutu, V. Eltsov, A. Gill, T. Kibble, M. Krusius, Y. G. Makhlin, B. Placais, G. Volovik, and W. Xu, *Nature* **382**, 334 (1996).

[31] M. J. Bowick, L. Chandar, E. A. Schiff, and A. M. Srivastava, *Science* **263**, 943 (1994).

[32] A. Maniv, E. Polturak, and G. Koren, *Physical review letters* **91**, 197001 (2003).

[33] C. N. Weiler, T. W. Neely, D. R. Scherer, A. S. Bradley, M. J. Davis, and B. P. Anderson, *Nature* **455**, 948 (2008).

[34] K. Staliunas and V. J. Sanchez-Morcillo, *Transverse patterns in nonlinear optical resonators*, Vol. 183 (Springer Science & Business Media, 2003).

[35] I. S. Aranson and L. Kramer, *Reviews of Modern Physics* **74**, 99 (2002).

[36] L. Carr and C. W. Clark, *Physical Review A* **74**, 043613 (2006).

[37] P. G. Kevrekidis, D. J. Frantzeskakis, and R. Carretero-González, *Emergent nonlinear phenomena in Bose-Einstein condensates: theory and experiment*, Vol. 45 (Springer Science & Business Media, 2007).

[38] N. G. Berloff and C. F. Barenghi, *Physical review letters* **93**, 090401 (2004).

[39] Fourth order Runge-Kutta integration is used. The initial wavefunction is set to a profile of low amplitude random noise. All simulations are repeated for many of these profiles.

[40] A. Askitopoulos, L. Pickup, S. Alyatkin, A. Zasedatelev, K. G. Lagoudakis, W. Langbein, and P. G. Lagoudakis, arXiv preprint arXiv:1911.08981 (2019).

[41] A. Amo, D. Sanvitto, F. Laussy, D. Ballarini, E. Del Valle, M. Martin, A. Lemaitre, J. Bloch, D. Krizhanovskii, M. Skolnick, *et al.*, *Nature* **457**, 291 (2009).

[42] Y. Kawaguchi and T. Ohmi, *Physical Review A* **70**, 043610 (2004).

[43] B. P. Abbott, R. Abbott, T. Abbott, F. Acernese, K. Ackley, C. Adams, T. Adams, P. Addesso, R. Adhikari, V. Adya, *et al.*, *Physical Review Letters* **119**, 161101 (2017).

[44] W. G. Unruh, *Physical Review Letters* **46**, 1351 (1981).

[45] G. E. Volovik, *The universe in a helium droplet*, Vol. 117 (Oxford University Press on Demand, 2003).

[46] J. Steinhauer, *Nature Physics* **10**, 864 (2014).

[47] N. Berloff and B. V. Svistunov, *Physics* **2**, 61 (2009).

[48] G. E. Volovik, *Journal of Experimental and Theoretical Physics Letters* **75**, 418 (2002).

[49] H. Takeuchi, N. Suzuki, K. Kasamatsu, H. Saito, and M. Tsubota, *Physical Review B* **81**, 094517 (2010).

[50] R. Hänninen and A. W. Baggaley, *Proceedings of the National Academy of Sciences* **111**, 4667 (2014).

[51] P. M. Lushnikov and N. M. Zubarev, *Physical review letters* **120**, 204504 (2018).